SHORT COMMUNICATION

MYCN induces neuroblastoma in primary neural crest cells

RR Olsen[1], JH Otero[1], J García-López[1], K Wallace[1], D Finkelstein[2], JE Rehg[3], Z Yin[1], Y-D Wang[2] and KW Freeman[1]

Neuroblastoma (NBL) is an embryonal cancer of the sympathetic nervous system (SNS), which causes 15% of pediatric cancer deaths. High-risk NBL is characterized by N-Myc amplification and segmental chromosomal gains and losses. Owing to limited disease models, the etiology of NBL is largely unknown, including both the cell of origin and the majority of oncogenic drivers. We have established a novel system for studying NBL based on the transformation of neural crest cells (NCCs), the progenitor cells of the SNS, isolated from mouse embryonic day 9.5 trunk neural tube explants. Based on pathology and gene expression analysis, we report the first successful transformation of wild-type NCCs into NBL by enforced expression of N-Myc, to generate phenotypically and molecularly accurate tumors that closely model human *MYCN*-amplified NBL. Using comparative genomic hybridization, we found that NCC-derived NBL tumors acquired copy number gains and losses that are syntenic to those observed in human *MYCN*-amplified NBL including 17q gain, 2p gain and loss of 1p36. When p53-compromised NCCs were transformed with N-Myc, we generated primitive neuroectodermal tumors with divergent differentiation including osteosarcoma. These subcutaneous tumors were metastatic to regional lymph nodes, liver and lung. Our novel experimental approach accurately models human NBL and establishes a new system with potential to study early stages of NBL oncogenesis, to functionally assess NBL oncogenic drivers and to characterize NBL metastasis.

INTRODUCTION

Neuroblastoma (NBL) is the most common extracranial pediatric solid tumor and is responsible for 15% of pediatric cancer deaths. It is a cancer of the sympathetic nervous system (SNS) with primary lesions found in the sympathetic ganglia and the adrenal medulla. Both clinical observations and treatment approaches suggest that NBL is a cancer caused by impaired development. Patients receive retinoic acid treatment as a standard therapy to promote tumor cell differentiation and a delayed onset of development is a prominent explanation for complete spontaneous regression seen in the 4S category of metastatic NBL. Furthermore, poorly differentiated/undifferentiated histology is an independent indicator of poor outcome for NBL.[1] From these observations, a block in development is thought to contribute to NBL oncogenesis.[2,3]

During development, neural crest cells (NCCs) are the precursor stem cell population that gives rise to neuroblasts, a proliferative post-migratory neural crest population that is a proposed cell of origin for NBL. NCCs are a highly migratory, multipotent cell population specified during neural tube closure that generate a variety of ectodermal and mesodermal tissues including neurons of the SNS, Schwann cells, melanocytes and osteoblasts.[4] NCCs migrate ventrally at mouse embryonic day 9.5 to the dorsal aorta where they receive inductive signals to form sympathetic ganglia or continue to the adrenal anlage to form chromaffin cells of the adrenal medulla. NCCs are the proposed embryonic precursor cell population to multiple pediatric malignancies including NBL, peripheral primitive neuroectodermal tumors, malignant peripheral nerve sheath tumors, craniofacial osteosarcoma, as well as adult malignancies such as melanoma.[3,5,6] However, primary NCCs have not been used to model any of these various malignancies.

N-Myc amplification and segmental chromosomal changes are the most frequent genetic alterations in high-risk NBL. However, the oncogenes and tumor suppressors from each of these segmental chromosomal gains and losses have not been defined, making the molecular etiology of this disease not well understood. Therefore, most modeling of the disease in mammalian systems is based on N-Myc overexpression.[7–10] In this study we establish a system for rapid, functional assessment of candidate oncogenic drivers in a normal genetic background and report the first successful transformation of primary NCCs into NBL by N-Myc overexpression. The resulting tumors both histologically and molecularly recapitulated *MYCN*-amplified NBL, including acquisition of chromosomal aberrations in regions syntenic to those seen in human N-Myc-amplified NBL. The NCC approach we have established is a promising new tool to assess the functional contribution of candidate oncogenic drivers and to study the role of impaired development in NBL tumorigenesis.

RESULTS AND DISCUSSION

Isolation and characterization of primary NCCs

Trunk NCCs migrate ventrally from the neural tube to form sympathetic ganglia and the adrenal medulla.[11] To isolate NCCs, trunk neural tube explants were dissected from 9.5 dpc embryos and cultured for 48 h, to allow NCC migration onto the plate. Isolated NCCs were then assessed by immunofluorescence and found to be uniformly positive for the early neural crest marker Sox10 and the p75 nerve growth factor receptor (Figure 1a).[12–14]

[1]Oncology Department, St. Jude Children's Research Hospital, Memphis, TN, USA; [2]Computational Biology Department, St. Jude Children's Research Hospital, Memphis, TN, USA and [3]Pathology Department, St. Jude Children's Research Hospital, Memphis, TN, USA. Correspondence: Dr KW Freeman, Oncology Department, St. Jude Children's Research Hospital 262 Danny Thomas Place, MS 354, Room D5048C Memphis, TN, 38105-3678, USA.
E-mail: kevin.freeman@stjude.org

We used quantitative PCR to compare gene expression in isolated NCCs versus adult mouse adrenal gland. As expected, NCCs had significantly higher levels of the neural crest markers Sox10, p75 and Ascl1 than adrenal gland (Figure 1b), but did not express Phox2B or TH, a marker for differentiated dopaminergic neurons (Figure 1c). These results indicate the isolated cells are uncommitted NCCs. When cells were cultured in neuronal differentiation media for 1 week, they generated neurons as determined by morphology (Figure 1d) and the neuronal marker MAP2 (microtubule-associated protein 2) (Figure 1e). Schwann cells were also generated among the neurons, as determined by GFAP (glial fibrillary acidic protein) immunostaining (Figure 1e). Both the marker analysis and the lineage commitment study confirmed that we are isolating highly enriched primary NCCs.

Compromised p53 with N-Myc leads to neuroectodermal tumors with divergent differentiation from NCCs

Aberrant N-Myc expression is found in NBL and N-Myc over-expression was used to model NBL in the TH-MYCN NBL mouse model; therefore, we tested the capacity of N-Myc to transform NCCs. We used *Trp53*-compromised NCCs to increase the likelihood of generating tumors with N-Myc transformation, as relatively few cells are isolated per neurotube explant (~3,000 NCCs) and there was no precedent for generating cancers from primary NCCs. To generate p53 compromised NCCs, we crossed p53-null males with p53 heterozygous females and isolated neurotube explants. NCCs pooled from both heterozygous and homozygous p53-null C57Bl/6 embryos were transduced with N-Myc-IRES-GFP retrovirus.[15] These N-Myc transduced cells are a

Oncogene (2017) 5075 – 5082
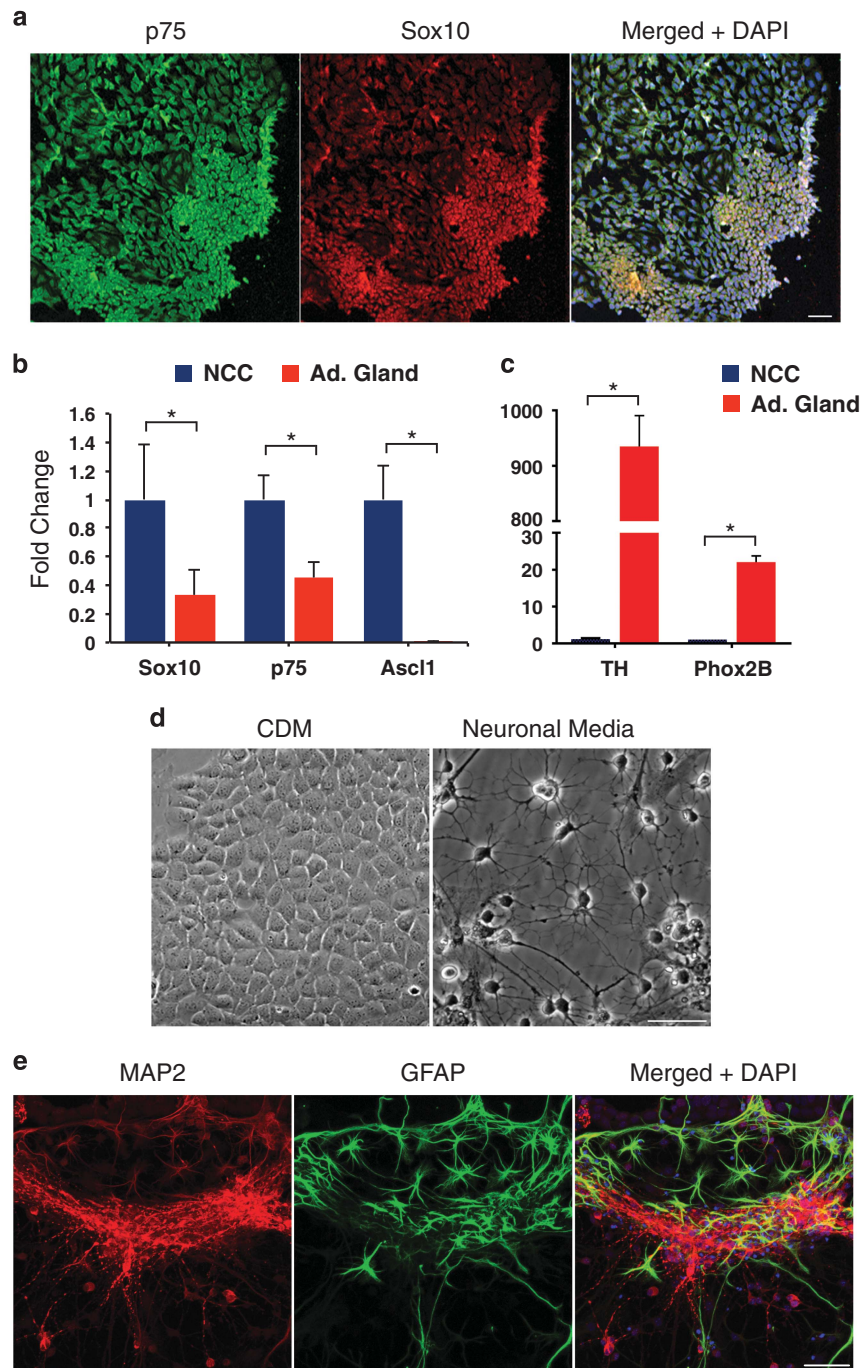
mixture of both p53$^{+/-}$ and p53$^{-/-}$ NCCs and are designated as N-Myc; p53^{mixed}. At 48 h post infection, N-Myc; p53^{mixed} NCCs were harvested and ~ 10,000 cells were injected subcutaneously into nude mice or into C57Bl/6 mice.

We observed 100% tumor penetrance with eight of eight tumors in the nude mice recipient cohort (Figure 2a, left panel) and six of six mice in the C57Bl/6 recipient cohort (Figure 2a, middle panel). There was a 50-day delay in mean tumor onset (tumors > 200 mm^3) observed in the immune-competent C57Bl/6 mice over the immune-compromised NU/NU mice. We also tested the ability of N-Myc to transform p53 heterozygous NCCs (N-Myc; p53$^{+/-}$) and found these cells generated tumors in four out of four mice (Figure 2a, right panel). None of the mice (0 out of 5 mice) injected with control p53^{mixed} NCCs infected with empty vector MSCV virus developed tumors as of 365 days post injection. Tumors from both the N-Myc; p53^{mixed} and the N-Myc;p53$^{+/-}$ NCCs displayed a mixed cancer phenotype for each tumor, although a subset were almost exclusively neuronal. Most tumor tissue was broadly positive for the neuronal marker synaptophysin. MAP2, Phox2B and TH were seen sporadically within the synaptophysin-positive regions of the tumors (Figure 2b). Tumors also had varying degrees of neuropil and ganglion-like features, which are both aspects of NBL.[16]

The next identifiable cancer type within the tumor mass was osteosarcoma with osteoid secretions and a subset of those osteosarcomas showed chondrocyte differentiation (Figure 2b, upper right). Additional malignancies that did not express any of the markers tested were also observed. Overall, by immunohistochemistry and pathology review tumors were characterized as primitive neuroectodermal tumors with divergent differentiation. In mice with slower growing tumors we noted macroscopic metastases. The metastases were observed in the lymph nodes, liver and lung, and often showed a mixed morphology similar to the primary tumors with regions of primitive neuroectodermal tumors and osteosarcoma (Figure 2c), although some lymph node metastases appeared exclusively NBL-like or osteosarcoma (Figure 2c, insets i and ii, respectively). Although TP53 is not found mutated at NBL diagnosis and rarely mutated at relapse, 49% of relapse patients showed defects in pathways upstream of p53, such as in p14^{ARF} and MDM2.[17,18] N-Myc overexpression in p53-compromised NCCs caused complete tumor penetrance and generated multiple cancer types. These results underscore the capacity of NCCs to generate a diverse array of cancer types, which corresponds to their capacity to generate a diverse array of tissues. Although subcutaneous tumors rarely metastasize, this was a salient feature of our neural crest-derived cancers, which recapitulates the highly metastatic nature of human NCC-derived cancers such as NBL and melanoma.

N-Myc transformation of NCCs generates NBL and osteosarcoma

Having established that tumors can be generated in our protocol, we next determined whether N-Myc was sufficient for transformation. NCCs were retrovirally infected within 48 h of isolation with either MSCV-NMyc-GFP or -RFP and cells were injected the next day subcutaneously into the flanks of mice. N-Myc NCCs generated tumors in 8 out of 26 (31%) mice with a broad range of tumor onsets from 52 days to 226 days (Figure 3a). The histologically assessed N-Myc NCC tumors were either neuronal or osteosarcoma and did not show the mixed morphology observed in N-Myc; p53^{mixed} NCC tumors (Figure 3b).

The neuronal tumors (Figure 3c) were composed of a highly proliferative homogeneous population with > 90% of the cells expressing nuclear Ki67 and diffuse Synaptophysin expression. The tumors were interspersed with neuropil, which indicates a poorly differentiated NBL. TH and MAP2 expression was seen in a scattering of individual cells and Chromogranin A expression was associated with ganglion-like cells adjacent to areas of necrosis. Phox2B, a highly specific and sensitive marker of NBL, was broadly expressed in the tumors.[19,20] N-Myc NCC tumors and N-Myc; p53^{mixed} NCC tumors had similar N-Myc mRNA expression levels to cultured N-Myc-transduced NCCs (N-Myc NCC), but much higher expression than non-transduced NCCs or adrenal medulla (Figure 3d). N-Myc protein expression for N-Myc NCC tumors was comparable to the TH-MYCN mouse model of NBL, whereas N-Myc; p53^{mixed} NCC tumors were comparable to dramatically higher expression of N-Myc (Figure 3e). Based on a pathologist's review of the tumors, they are consistent with a classification of large cell/nucleolar NBL of the poorly differentiated subtype.[16,21] The large cell/nucleolar NBL subclassification of neuroblastoma is strongly associated with N-Myc amplification and is speculated to be a consequence of N-Myc overexpression.[16,21] This subtype is also a highly aggressive variant of NBL with very poor outcome that is proposed to be a developmentally immature stem cell-like NBL.[21,22]

The second set of tumors was negative for Synaptophysin, Phox2B, Map2, TH and Chromogranin A. By hematoxylin and eosin staining, the tumors showed features of osteosarcoma with extensive osteoid throughout the tumors and were designated as osteosarcomas (Figure 3b, right). During craniofacial development, NCC-derived osteoblasts form the bone and cartilage of the face and neck. Mutations in p53 are frequently observed in human osteosarcoma; similarly, we found that the N-Myc osteosarcoma

---

Figure 1. Cells isolated from trunk neural tube explants are NCCs by marker analysis and differentiation potential. (**a**) Day 9.5 embryos were isolated and dissected to remove the neural tube from a region caudal to the heart to the most caudal somite. Isolated neural trunks were treated with 1 mg/ml collagenase/dispase for 5 min, while being triturated in a Pasteur pipette. Neural tube explants were cultured in neural crest media (EMEM (Life Technologies, Waltham, MA, USA, 51200-038) with 3% chick embryo extract (US Biologicals, Salem, MA, USA, C3999) and 15% fetal bovine serum (Omega Scientific, Tarzana, CA, USA, FB-02)) on fibronectin-coated plates for 48 h, to allow NCC migration onto the plate before the neural tubes were removed. Immunofluorescence staining on cells isolated from neural tube explants using antibodies to the nerve growth factor receptor p75 (green, EMD Millipore, Billerica, MA, USA, 07-476) and the transcription factor Sox10 (red, ThermoFisher Scientific, Waltham, MA, USA, MAB2864), both markers of early neural crest. The merged image also includes DAPI nuclear staining. Scale bar = 10 μm. (**b**) Quantitative real-time PCR was performed on a 7900HT Real Time PCR Machine (Applied Biosystems, Waltham, MA, USA) using Taqman Fast Advanced Master Mix (Life Technologies, 4444965). Expression of the early neural crest markers p75 and Sox10, and the migratory neural crest marker Ascl1 were measured relative to B2M in isolated NCCs compared with adult mouse adrenal gland, a differentiated SNS tissue (n = 2–3). *P < 0.001. (**c**) Quantitative real-time PCR comparing expression of Tyrosine hydroxylase (a marker of differentiated SNS) and Phox2B (an SNS lineage marker) in isolated NCCs versus adrenal gland tissue (n = 2–3). *P < 0.01. Results are expressed as the mean ± s.d. We utilized a two-tail, unpaired Student's t-test for all pair-wise comparisons (GraphPad Prism version 6) and analysis of variance where appropriate (GraphPad Prism). P-values < 0.05 were considered statistically significant. TaqMan primers and probes (ThermoFisher Scientific) used include the following: p75 (Mm01309638_m1), Sox10 (Mm01300162_m1), Ascl1 (Mm04207567_g1), TH (Mm00447557_m1), Phox2B (Mm00435872_m1) and B2M (Mm0437762_m1). (**d**) Bright-field images of NCCs grown in chemically defined media (CDM) or neuronal differentiation media[35] for 1 week. Scale bar = 50 μm. (**e**) Immunofluorescence staining for markers of neurons (MAP2, Abcam, Cambridge, MA, USA, ab5392) and glia (GFAP, Cell Signaling Technology, Danvers, MA, USA, XP12389P) following differentiation of NCCs in neuronal differentiation media for 1 week. The merged image also includes DAPI nuclear staining. Scale bar = 50 μm.
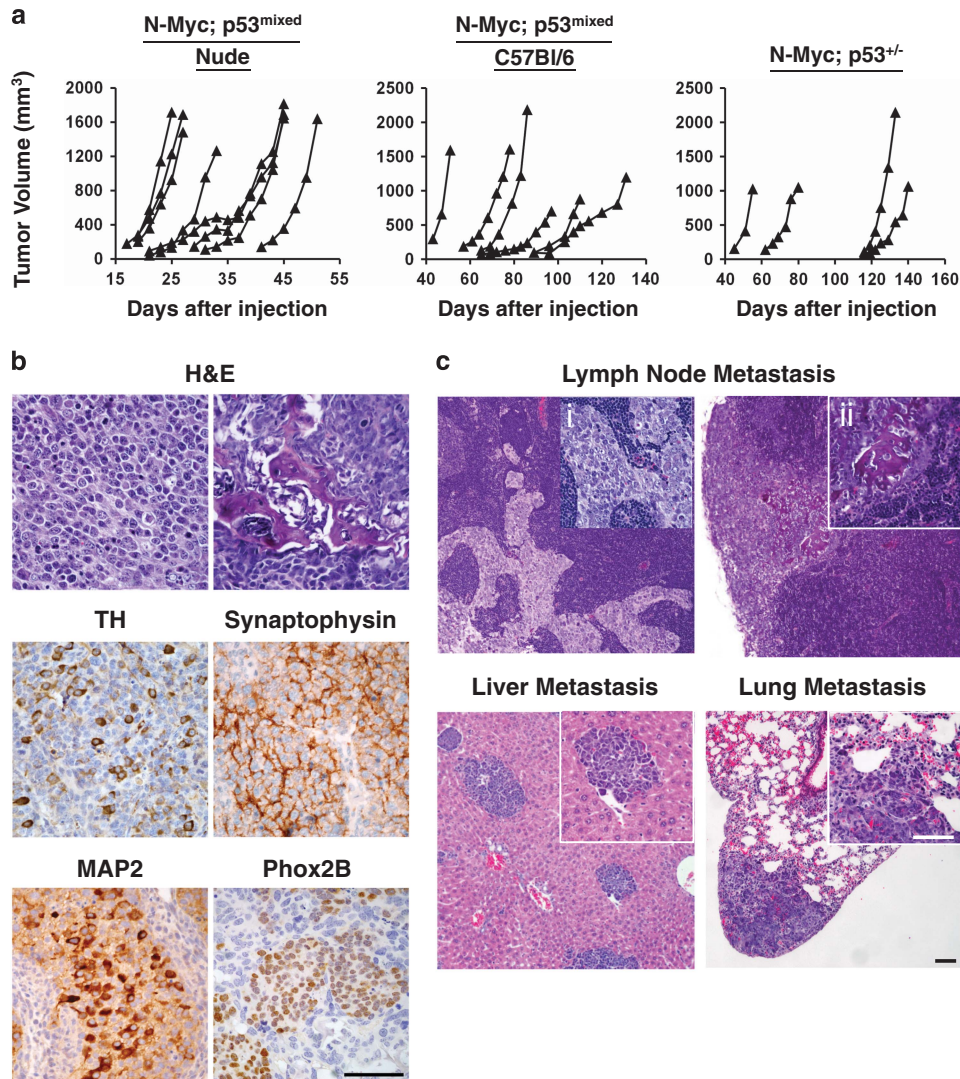
Figure 2. N-Myc transforms p53 compromised NCCs into metastatic primitive neuroectodermal tumors with divergent differentiation. (**a**) Approximately 10,000 p53[mixed] or p53^{+/−} NCCs infected with N-Myc virus[36] were mixed with 100 µl Matrigel (BD Biosciences, San Jose, CA, USA, 356237) and injected subcutaneously on the right flank of 6- to 8-week-old either Nu/Nu mice or C57Bl/6 mice (Charles River, Wilmington, MA, USA). Mice were injected on a rolling basis, to generate sufficient numbers of tumors for further analysis in a non-randomized, non-blinded manner. Eight Nu/Nu mice (left panel) and six C57Bl/6 mice (middle panel) were each flank injected with N-Myc transduced primary p53[mixed] NCCs pooled from p53^{+/−} and p53^{−/−} embryos (middle panel). Four C57Bl/6 mice were flank injected with N-Myc transduced primary p53^{+/−} NCCs (right panel). Individual tumor volumes were measured over time as previously described.[36] (**b**) Formalin-fixed tissue samples were prepared as previously described.[36] Representative tumor histology (hematoxylin and eosin, H&E) is shown from a region positive for neuronal markers (upper left) and a region with osteosarcoma (upper right). Representative immunohistochemistry images show expression of neuronal markers. Antibodies used include TH (1:40, Vector, Burlingame, CA, USA, VP-T489), Synaptophysin (1:100, Spring Biosciences, Pleasanton, CA, USA, E2172), MAP2 (1:250, Millipore, Billerica, MA, USA, AB5622) and Phox2B (1:100, Abcam, ab183741). Scale bars = 50 µm. (**c**) Representative histology (H&E) of lymph node, liver and lung metastasis with areas of metastasis highlighted in the insets. Scale bars = 50 µm. This experiment was performed in strict accordance with the recommendations in the Guide for the Care and Use of Laboratory Animals of the National Institute of Health. Mice were sacrificed using CO_2 asphyxiation followed by cervical dislocation. This research was approved by the St. Jude Children's Research Hospital IACUC.

tumors had acquired p53 mutations including S209R or K126T (data not shown). This work establishes that primary NCCs when transduced with N-Myc generate NBL and additionally when p53 is mutated can generate osteosarcoma.

Gene expression analysis shows NCC-derived N-Myc tumors represent molecularly accurate NBL

The N-Myc and N-Myc; p53[mixed] NCC tumors were assayed by quantitative PCR for expression of the NBL markers *Phox2b* and *TH* as well as osteosarcoma markers *Runx2* and *Satb2* (Supplementary Figure 1). Although neuroblastma tumors were the majority of

N-Myc NCC tumors, they represented a minority of N-Myc; p53[mixed] NCC tumors (Supplementary Figure 2). Three *Phox2b/ TH*-positive, *Runx2/Satb2*-negative N-Myc NCC tumors were submitted for gene expression analysis using Affymetrix Mouse 2.0 ST arrays (ThermoFisher Scientific, Waltham, MA, USA). Genes found upregulated > 2 log ratio over normal adrenal for the mouse NCC-derived NBL were analyzed with the Cancer Cell Line Encyclopedia database using the gene set analysis tool Enrichr.[23,24] The N-Myc NCC tumors matched human NBL at an average significance of *P*-value $< 1 \times 10^{-7}$ (Figure 4a). When NCC-derived NBL were compared with individual NBL cell lines, the NCC-derived NBL tumors best fit with N-Myc amplified NBL with *P*-
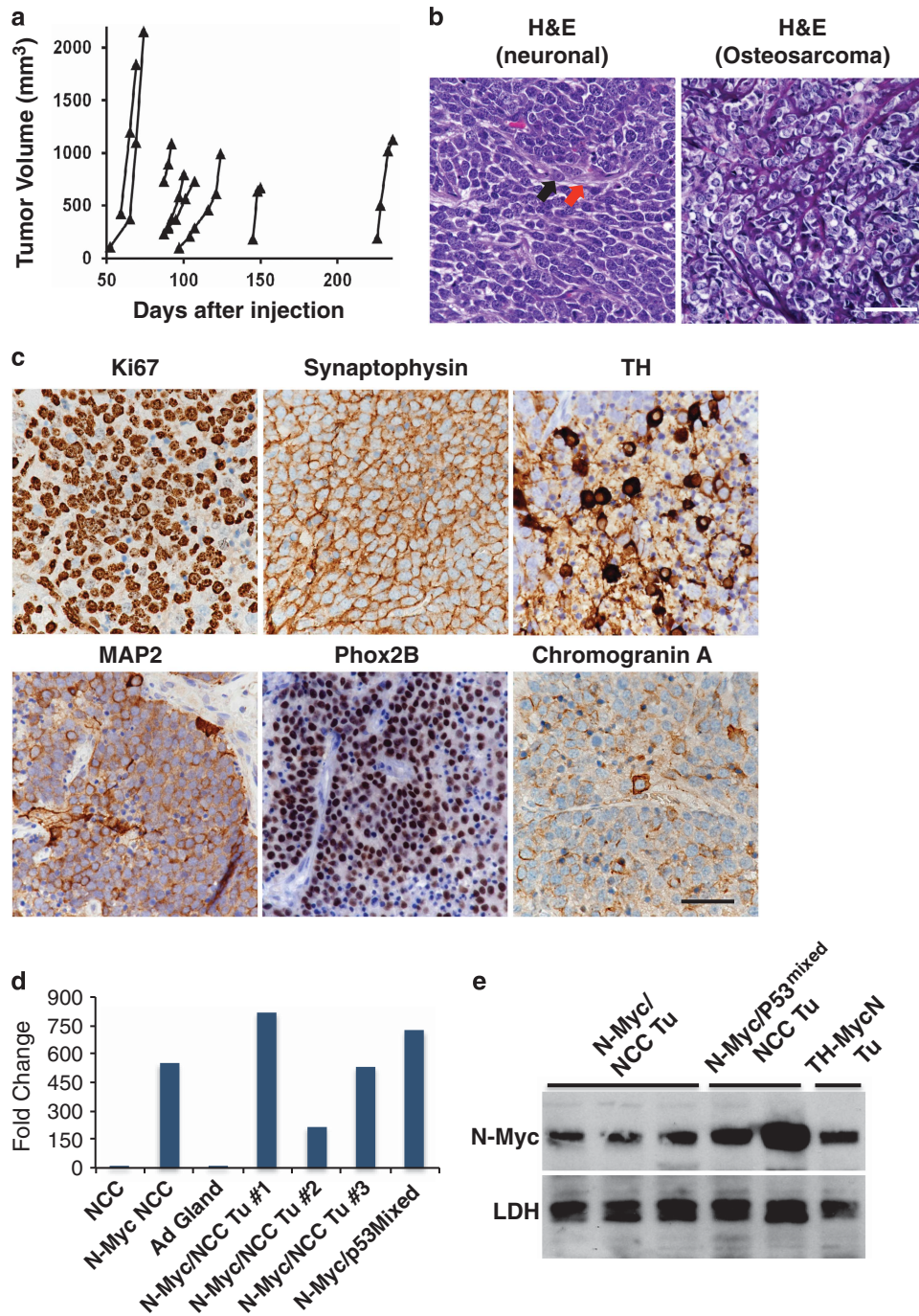
Figure 3. N-Myc transforms primary NCCs into NBL. (**a**) Approximately 10 000 wild-type NCCs infected with N-Myc were mixed with 100 ul Matrigel (BD Biosciences, 356237) and injected subcutaneously on the right flank of 6- to 8-week-old either Nu/Nu mice or C57Bl/6 mice (Charles River). Mice were injected on a rolling basis to generate sufficient numbers of tumors for further analysis in a non-randomized, non-blinded manner. Mice were killed and tumors isolated when they were at least 1000 mm³ or earlier if ulcerated. A total of 26 mice were flank injected with N-Myc transduced primary NCCs. (**b**) Representative hematoxylin and eosin (H&E) tumor histology from NCC tumors that were uniformly neuronal (left) or osteosarcoma (right). The black arrow identifies a ganglion cell and the red arrow identifies neuropil. Scale bar = 50 μm. (**c**) Representative immunohistochemistry (IHC) images of neuronal tumors stained for Ki67 (1:200, ThermoFisher Scientific, RM-9106), Synaptophysin, TH, MAP2, Phox2B and Chromogranin A (1:1500, Immunostar, Hudson, WI, USA). Scale bar = 50 μm. (**d**) Quantitative real-time PCR was performed on primary NCC, N-Myc virally transduced NCCs (N-Myc NCC), N-Myc NCC tumors (N-Myc/NCC Tu) and N-Myc; p53^{mixed} NCC tumors (N-Myc; p53^{mixed} NCC Tu) for NMYC (Mm00476449_m1) gene expression. Values indicate fold change over N-Myc expression in NCC, which is set at 1. (**e**) Protein was extracted from tumors derived from N-Myc NCCs and N-Myc; p53^{mixed} NCCs, as well as isolated from the TH-MYCN mouse model of NBL by homogenizing with T-PER buffer (ThermoFisher Scientific) using a MicroTube homogenizer. Blots were probed with antibodies for N-Myc (Cell Signaling Technologies 9405) and as loading control lactate dehydrogenase (Abcam ab47010). Rabbit secondary (Cell Signaling Technologies 7074) and ECL Select (Amersham, Pittsburgh, PA, USA) were used to detect the signals. This experiment was performed in strict accordance with the recommendations in the Guide for the Care and Use of Laboratory Animals of the National Institute of Health. Mice were sacrificed using CO_2 asphyxiation followed by cervical dislocation. This research was approved by the St. Jude Children's Research Hospital IACUC.
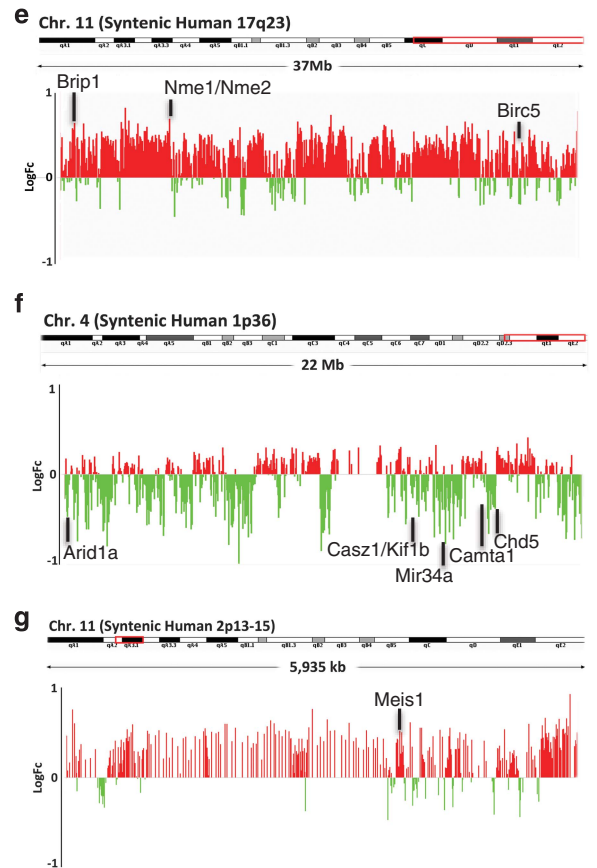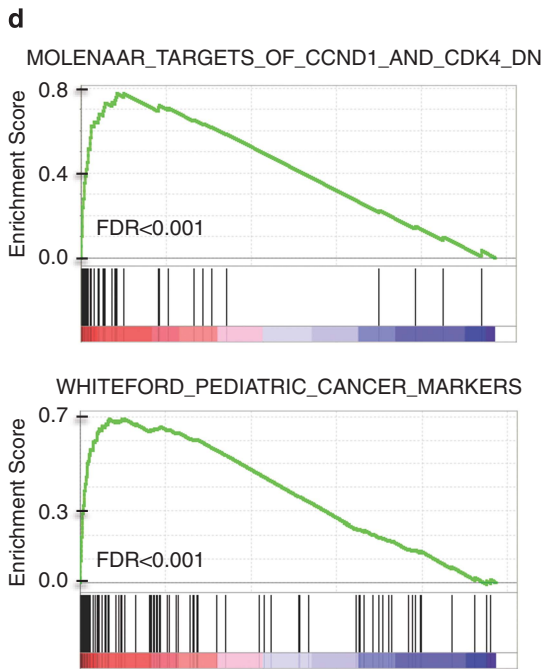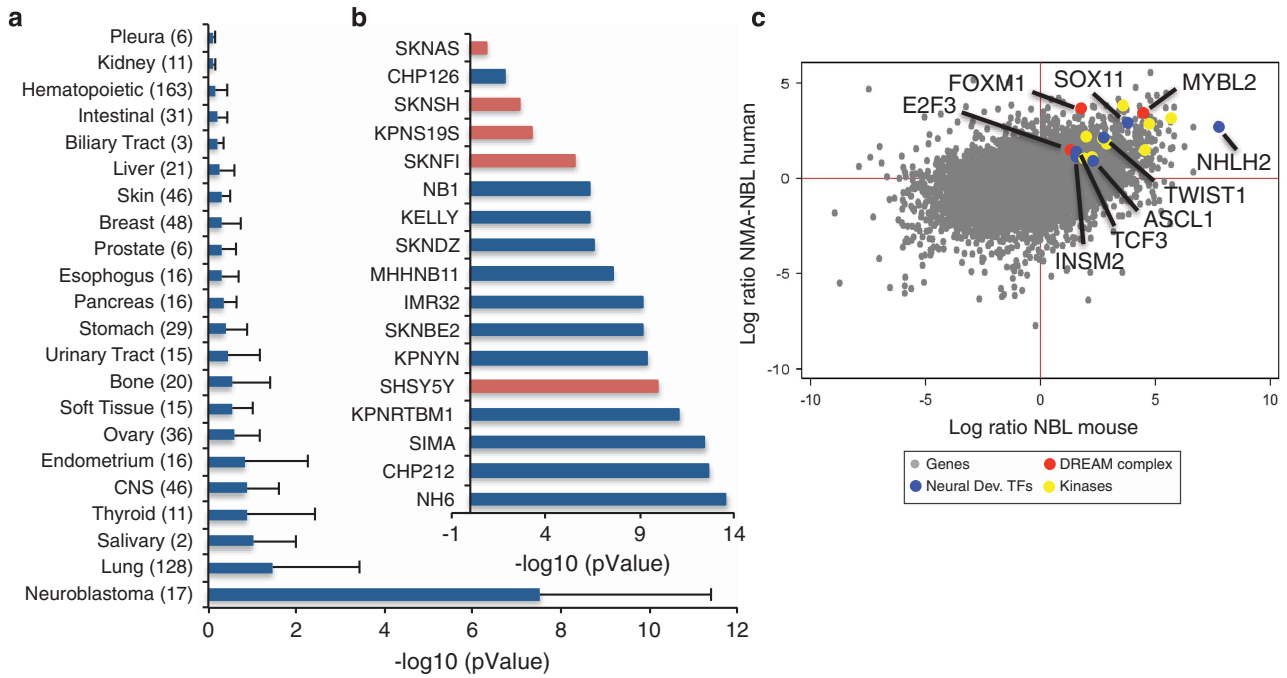
value $< 1 \times 10^{-13}$ (Figure 4b). Both pathology and gene set analysis indicate the N-Myc NCC-derived NBL recapitulates *MYCN*-amplified NBL.

To identify commonly upregulated genes that might be important for NBL oncogenesis, we compared the gene expression profile of the N-Myc NCC NBLs with human N-Myc-amplified NBLs. Genes with interspecies gene expression >1 log ratio for mouse and human NBL tumors over normal adrenal were determined (Figure 4c). *Foxm1*, *Mybl2* (BMYB) and *E2f3* are all highly overexpressed in both the human and mouse NBL (Figure 4c), and are part of a cell cycle regulatory complex. During proliferation, the multi-vulval class B (MuvB) protein complex regulates progressive stages of the cell cycle through coordinated interactions with B-MYB (*Mybl2*) and forkhead M1 (*Foxm1*).[25] In

addition to upregulating E2F1-3, Myc transcription factors also upregulate many of the cell-cycle targets of the BMYB–MuvB–FOXM1 complex. Further, both Foxm1 and B-Myb have been shown to be important oncogenic factors in NBL cell lines, with B-Myb showing a reciprocal regulatory loop with N-Myc.[26,27] Enrichment plots of differentially expressed gene signatures in N-Myc NCC tumors versus adrenal medulla using gene set enrichment analysis tools and the Molecular Signature Database (Broad Institute, Cambridge, MA, USA) also identified targets of the cell cycle genes CCND1 and CDK4 in NBL primary tumors and shared pediatric cancer markers (Figure 4d). Additional gene set enrichment analysis identified molecular signatures for E2F3 targets, Myc targets, BMYB–MuvB–FOXM1 complex targets from the MuvB subunit Lin9 signature and MycN targets in NBL tumors (Versteeg NB88) (Supplementary Figure 3).

In addition to the upregulated cell-cycle-associated genes, both human NBL and NCC-derived NBL shared multiple upregulated neural developmental transcription factors (Sox11, Nhlh2, Twist1, Ascl1, Insm2 and Tcf3) that are also important for neural crest development. TCF3 is a bHLH protein that partners with tissue-specific bHLH transcription factors to transactivate target genes and is known to interact with both Twist1 and Ascl1. Phox2b and Ascl1 regulate Hand 1/2 and Gata 2/3, which promote sympathoa-drenal differentiation and proliferation. Both Twist1 and Ascl1 are direct transcriptional targets of N-Myc[28,29] and all three of these transcription factors, along with Nhlh2, have been shown to be important in NBL oncogenesis.

Although direct therapeutic targeting of transcription factors is difficult, their downstream effectors, such as kinases, are potential drug targets. We identified multiple kinases that show shared overexpression between our model and human NBL (Figure 4c and Supplementary Figure 4). Some of these kinases have already been shown to be promising targets in NBL, including anaplastic lymphoma receptor tyrosine kinase, check-point kinase 1 and aurora kinase A.[30–32] Our data highlights additional kinases that may be important therapeutic targets including cyclin-dependent kinase-1 and PDZ-binding kinase. Inhibitors to cyclin-dependent kinase-1 are currently in clinical trials[33] and PDZ-binding kinase is overexpressed in many cancers and correlates with poor prognosis in various malignancies. Small-molecule inhibitors of PDZ-binding kinase have shown promise in reducing growth of glioblastoma tumors in mice.[34] From N-Myc NCC tumors and N-Myc; p53[mixed] NCC tumors, we have established serially passaged tumor xenografts and tumor cell lines as a resource for testing promising therapies.

NCC-derived NBL recapitulates the chromosomal changes seen in N-Myc-amplified NBL

Based on quantitative PCR analysis (Supplementary Figure 1), five Phox2b-positive, Runx2/Satb2-negative N-Myc NCC and N-Myc p53[mixed] NCC tumors were submitted for array comparative genomic hybridization to identify chromosomal alterations. Compared with normal mouse liver genomic DNA, NCC-derived tumors recapitulated many of the chromosomal gains and losses observed in human MYCN-amplified NBL. Specifically, we observed at least three out of five NCC-derived tumors with amplification of regions syntenic to human 17q (Figure 4e), loss of regions syntenic to human 1p36 (Figure 4f) and gain of regions syntenic to human 2p13-15 (Figure 4g). A full list of log2ratios for individual array comparative genomic hybridization probes in these regions is provided in Supplementary Table 1.

Our manuscript establishes that it is possible to isolate and ex vivo genetically manipulate NCCs to establish NBL tumors in mice. This more rapid method of generating mouse models of NBL is an important new way to interrogate the genetics of cancer in addition to the more traditionally used strategies of cell lines, xenografts and genetically engineered mouse models. Key challenges for NBL research are establishing the molecular etiology of this disease, defining the contribution of impaired development to NBL oncogenesis and finding tractable therapeutic targets. By successfully transforming primary NCC into NBL, we have created a new tool for investigating these critical questions in NBL research.

CONFLICT OF INTEREST

The authors declare no conflict of interest.

REFERENCES

1 Meany HJ, London WB, Ambros PF, Matthay KK, Monclair T, Simon T et al. Significance of clinical and biologic features in Stage 3 neuroblastoma: a report from the International Neuroblastoma Risk Group project. Pediatr Blood Cancer 2014; **61**: 1932–1939.

2 Wylie LA, Hardwick LJ, Papkovskaia TD, Thiele CJ, Philpott A. Ascl1 phospho-status regulates neuronal differentiation in a Xenopus developmental model of neuro-blastoma. Disease Models Mech 2015; **8**: 429–441.

3 Louis CU, Shohet JM. Neuroblastoma: molecular pathogenesis and therapy. Ann Rev Med 2015; **66**: 49–63.

4 Simoes-Costa M, Bronner ME. Establishing neural crest identity: a gene regulatory recipe. Development 2015; **142**: 242–257.

5082

5 Karunasena E, McIver LJ, Bavarva JH, Wu X, Zhu H, Garner HR. 'Cut from the same cloth': Shared microsatellite variants among cancers link to ectodermal tissues-neural tube and crest cells. *Oncotarget* 2015; **6**: 22038–22047.

6 Mahomed F, Rikhotso E. Ossifying fibroma in a patient with oculocerebrocutaneous (Delleman) syndrome. *J Oral Maxillofac Surg* 2015; **73**: 1314–1319.

7 Weiss WA, Aldape K, Mohapatra G, Feuerstein BG, Bishop JM. Targeted expression of MYCN causes neuroblastoma in transgenic mice. *EMBO J* 1997; **16**: 2985–2995.

8 Althoff K, Beckers A, Bell E, Nortmeyer M, Thor T, Sprussel A et al. A Cre-conditional MYCN-driven neuroblastoma mouse model as an improved tool for preclinical studies. *Oncogene* 2015; **34**: 3357–3368.

9 Schulte JH, Lindner S, Bohrer A, Maurer J, De Preter K, Lefever S et al. MYCN and ALKF1174L are sufficient to drive neuroblastoma development from neural crest progenitor cells. *Oncogene* 2013; **32**: 1059–1065.

10 Montavon G, Jauquier N, Coulon A, Peuchmaur M, Flahaut M, Bourloud KB et al. Wild-type ALK and activating ALK-R1275Q and ALK-F1174L mutations upregulate Myc and initiate tumor formation in murine neural crest progenitor cells. *Oncotarget* 2014; **5**: 4452–4466.

11 Huber K. Segregation of neuronal and neuroendocrine differentiation in the sympathoadrenal lineage. *Cell Tissue Res* 2015; **359**: 333–341.

12 Stemple DL, Anderson DJ. Isolation of a stem cell for neurons and glia from the mammalian neural crest. *Cell* 1992; **71**: 973–985.

13 Rao MS, Anderson DJ. Immortalization and controlled in vitro differentiation of murine multipotent neural crest stem cells. *J Neurobiol* 1997; **32**: 722–746.

14 Kim J, Lo L, Dormand E, Anderson DJ. SOX10 maintains multipotency and inhibits neuronal differentiation of neural crest stem cells. *Neuron* 2003; **38**: 17–31.

15 Kawauchi D, Robinson G, Uziel T, Gibson P, Rehg J, Gao C et al. A mouse model of the most aggressive subgroup of human medulloblastoma. *Cancer Cell* 2012; **21**: 168–180.

16 Tornoczky T, Kalman E, Kajtar PG, Nyari T, Pearson AD, Tweddle DA et al. Large cell neuroblastoma: a distinct phenotype of neuroblastoma with aggressive clinical behavior. *Cancer* 2004; **100**: 390–397.

17 Wolter J, Angelini P, Irwin M. p53 Family: therapeutic targets in neuroblastoma. *Future Oncol* 2010; **6**: 429–444.

18 Carr-Wilkinson J, O'Toole K, Wood KM, Challen CC, Baker AG, Board JR et al. High frequency of p53/MDM2/p14ARF pathway abnormalities in relapsed neuroblastoma. *Clin Cancer Res* 2010; **16**: 1108–1118.

19 Bielle F, Freneaux P, Jeanne-Pasquier C, Maran-Gonzalez A, Rousseau A, Lamant L et al. PHOX2B immunolabeling: a novel tool for the diagnosis of undifferentiated neuroblastomas among childhood small round blue-cell tumors. *Am J Surg Pathol* 2012; **36**: 1141–1149.

20 Hata JL, Correa H, Krishnan C, Esbenshade AJ, Black JO, Chung DH et al. Diagnostic utility of PHOX2B in primary and treated neuroblastoma and in neuroblastoma metastatic to the bone marrow. *Arch Pathol Lab Med* 2015; **139**: 543–546.

21 Tornoczky T, Semjen D, Shimada H, Ambros IM. Pathology of peripheral neuroblastic tumors: significance of prominent nucleoli in undifferentiated/poorly differentiated neuroblastoma. *Pathol Oncol Res* 2007; **13**: 269–275.

22 Ikegaki N, Shimada H, Fox AM, Regan PL, Jacobs JR, Hicks SL et al. Transient treatment with epigenetic modifiers yields stable neuroblastoma stem cells resembling aggressive large-cell neuroblastomas. *Proc Natl Acad Sci USA* 2013; **110**: 6097–6102.

23 Barretina J, Caponigro G, Stransky N, Venkatesan K, Margolin AA, Kim S et al. The Cancer Cell Line Encyclopedia enables predictive modelling of anticancer drug sensitivity. *Nature* 2012; **483**: 603–607.

24 Kuleshov MV, Jones MR, Rouillard AD, Fernandez NF, Duan Q, Wang Z et al. Enrichr: a comprehensive gene set enrichment analysis web server 2016 update. *Nucleic Acids Res* 2016; **44**: W90–W97.

25 Sadasivam S, Duan S, DeCaprio JA. The MuvB complex sequentially recruits B-Myb and FoxM1 to promote mitotic gene expression. *Genes Dev* 2012; **26**: 474–489.

26 Wang Z, Park HJ, Carr JR, Chen YJ, Zheng Y, Li J et al. FoxM1 in tumorigenicity of the neuroblastoma cells and renewal of the neural progenitors. *Cancer Res* 2011; **71**: 4292–4302.

27 Gualdrini F, Corvetta D, Cantilena S, Chayka O, Tanno B, Raschella G et al. Addiction of MYCN amplified tumours to B-MYB underscores a reciprocal regulatory loop. *Oncotarget* 2010; **1**: 278–288.

28 Valsesia-Wittmann S, Magdeleine M, Dupasquier S, Garin E, Jallas AC, Combaret V et al. Oncogenic cooperation between H-Twist and N-Myc overrides failsafe programs in cancer cells. *Cancer Cell* 2004; **6**: 625–630.

29 Watt F, Watanabe R, Yang W, Agren N, Arvidsson Y, Funa K. A novel MASH1 enhancer with N-myc and CREB-binding sites is active in neuroblastoma. *Cancer Gene Ther* 2007; **14**: 287–296.

30 Russell MR, Levin K, Rader J, Belcastro L, Li Y, Martinez D et al. Combination therapy targeting the Chk1 and Wee1 kinases shows therapeutic efficacy in neuroblastoma. *Cancer Res* 2013; **73**: 776–784.

31 Mosse YP, Lim MS, Voss SD, Wilner K, Ruffner K, Laliberte J et al. Safety and activity of crizotinib for paediatric patients with refractory solid tumours or anaplastic large-cell lymphoma: a Children's Oncology Group phase 1 consortium study. *Lancet Oncol* 2013; **14**: 472–480.

32 Schwermer M, Lee S, Koster J, van Maerken T, Stephan H, Eggert A et al. Sensitivity to cdk1-inhibition is modulated by p53 status in preclinical models of embryonal tumors. *Oncotarget* 2015; **6**: 15425–15435.

33 Asghar U, Witkiewicz AK, Turner NC, Knudsen ES. The history and future of targeting cyclin-dependent kinases in cancer therapy. *Nat Rev Drug Discov* 2015; **14**: 130–146.

34 Joel M, Mughal AA, Grieg Z, Murrell W, Palmero S, Mikkelsen B et al. Targeting PBK/TOPK decreases growth and survival of glioma initiating cells in vitro and attenuates tumor growth in vivo. *Mol Cancer* 2015; **14**: 121.

35 Fukuta M, Nakai Y, Kirino K, Nakagawa M, Sekiguchi K, Nagata S et al. Derivation of mesenchymal stromal cells from pluripotent stem cells through a neural crest lineage using small molecule compounds with defined media. *PLoS ONE* 2014; **9**: e112291.

36 Olsen RR, Mary-Sinclair MN, Yin Z, Freeman KW. Antagonizing Bcl-2 family members sensitizes neuroblastoma and Ewing's sarcoma to an inhibitor of glutamine metabolism. *PLoS ONE* 2015; **10**: e0116998.

Supplementary Information accompanies this paper on the Oncogene website (http://www.nature.com/onc)